Zak-OTFS based ISAC and Radar

Prof. Saif Khan Mohammed, I.I.T. Delhi, India

Collaborative work with
M. Ubadah and D. Nisar, I.I.T. Delhi,
R. Hadani, UT Austin USA, A. Chockalingam, I.I.Sc. Bangalore and
R. Calderbank, Duke University USA
(https://sites.google.com/view/prof-saif-khan-mohammed/research)

Department of Electrical and Computer Engineering
University of Texas at Austin, USA

6 June, 2025

Zak-OTFS Modulation - A Review

Zak-OTFS Modulation

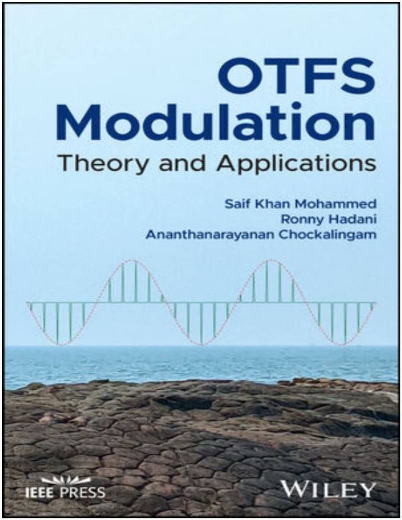

- So far no corresponding theory for reliable communication in doubly-spread channels – Considered to be an old challenging problem
- We have pioneered a Zak-transform based theory for reliable communication in doubly-spread channels
- Delay-Doppler signal processing is expected to revolutionize the design of future communication and radar systems

Pulsones: A new basis for TD signals

- The well known periodic impulse train

$$p_{0,0}(t) \quad = \quad \sqrt{\tau_p} \sum_{k \in \mathbb{Z}} \delta(t - k\tau_p)$$

- $p_{0,0}(t)$ delay and Doppler shifted by (τ, ν)

$$p_{\tau,\nu}(t) \quad = \quad \sqrt{\tau_p}\, e^{j2\pi\nu(t-\tau)} \sum_{k \in \mathbb{Z}} \delta(t - \tau - k\tau_p)$$

- Pulsones $p_{\tau,\nu}(t)$, $(\tau, \nu) \in \mathbb{R}^2$ forms a basis for TD signals

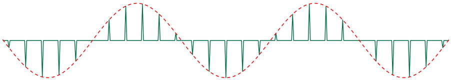

Pulsones and the Zak-transform

- Sinusoidal basis ($e^{j2\pi ft}$): Fourier transform is projection onto this basis, $X(f) = \int x(t)\, e^{-j2\pi ft}\, dt$.
- Zak-transform $\mathcal{Z}_t$: Projection of $x(t)$ on this basis

$$\begin{aligned} x_{\mathrm{dd}}(\tau,\nu) &\triangleq \mathcal{Z}_t\Big(x(t)\Big) = \int x(t)\, p^{*}_{\tau,\nu}(t)\, dt \\ &= \sqrt{\tau_p} \sum_{k\in\mathbb{Z}} x(\tau + k\tau_p)\, e^{-j2\pi k\nu\tau_p} \end{aligned}$$

- DD realizations are Quasi-periodic functions:

$$\begin{aligned} x_{\mathrm{dd}}(\tau + n\tau_p, \nu + m\nu_p) &= e^{j2\pi n\nu\tau_p}\, x_{\mathrm{dd}}(\tau,\nu), \;\; n, m \in \mathbb{Z} \\ \nu_p &\triangleq \frac{1}{\tau_p} \end{aligned}$$

- Pulsones form a basis: $x(t) = \int_0^{\tau_p} \int_0^{\nu_p} x_{\mathrm{dd}}(\tau,\nu)\, p_{\tau,\nu}(t)\, d\tau\, d\nu$

S. K. Mohammed, "Derivation of OTFS Modulation From First Principles," *IEEE Transactions on Vehicular Technology*, vol. 70, no. 8, pp. 7619-7636, Aug. 2021.

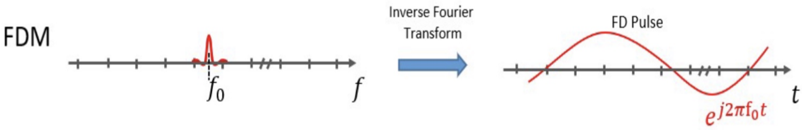

Figure: Fourier transform: $x(t) \leftrightarrow X(f)$, $x(t) = \int X(f)\, e^{j2\pi f\, t}\, df$

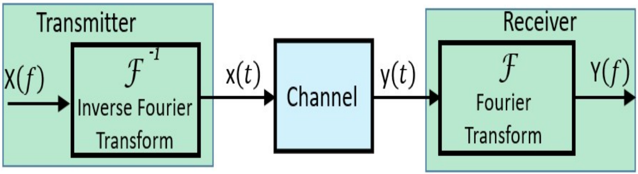

Figure: OFDM Tx. and Rx. signal processing in frequency domain (FD).

Pulsones:OTFS :: Sinusoids:OFDM

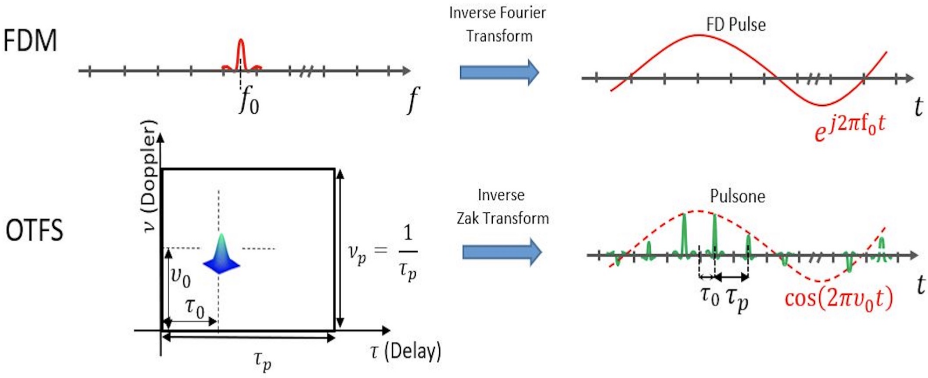

Figure: Zak transform: $x(t) \rightarrow x_{\text{dd}}(\tau, \nu)$, $x(t) = \int_0^{\tau_p} \int_0^{\nu_p} x_{\text{dd}}(\tau, \nu)\, p_{\tau,\nu}(t)\, d\tau\, d\nu$

Channel action

- Delay-only channels: Channel acts through linear convolution with its impulse response $y(t) = h(t) \star x(t)$. I/O relation is predictable if $h(t)$ is stationary
- Doubly-spread channels: Channel acts on the DD representation of input through *twisted convolution* with its DD spreading function

$$y(t) = \iint h(\tau', \nu')\, x(t - \tau')\, e^{j2\pi\nu'(t-\tau')}\, d\tau'\, d\nu'$$

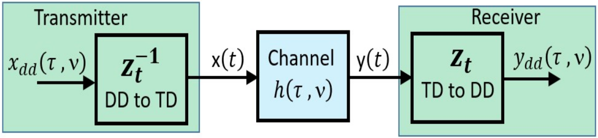

$$y_{dd}(\tau, \nu) = h(\tau, \nu) *_\sigma x_{dd}(\tau, \nu)$$

$$x(t) \rightarrow x_{dd}(\tau, \nu) \;\equiv\; x(t - \tau')\, e^{j2\pi\nu'(t-\tau')} \;\rightarrow\; x_{dd}(\tau - \tau', \nu - \nu')\, e^{j2\pi\nu'(\tau-\tau')}$$

$$y_{dd}(\tau, \nu) = \iint h(\tau', \nu')\, x_{dd}(\tau - \tau', \nu - \nu')\, e^{j2\pi\nu'(\tau-\tau')}\, d\tau'\, d\nu'$$

Pulsone is a Quasi-periodic pulse in DD domain

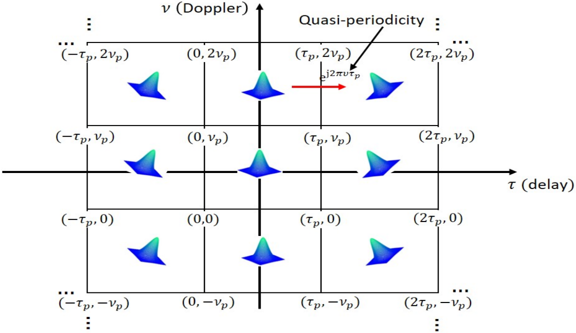

- Quasi-periodic DD pulse: delay period τ_p, Doppler period $\nu_p = 1/\tau_p$
- Pulse *effectively* localized in the fundamental DD period: $\mathcal{D}_0 \triangleq \left\{(\tau, \nu) \,\middle|\, 0 \leq \tau < \tau_p,\ 0 \leq \nu < \nu_p \right\}$
- Information carrier for Zak-OTFS modulation

*Figure taken from [4].

Zak-OTFS carrier waveform

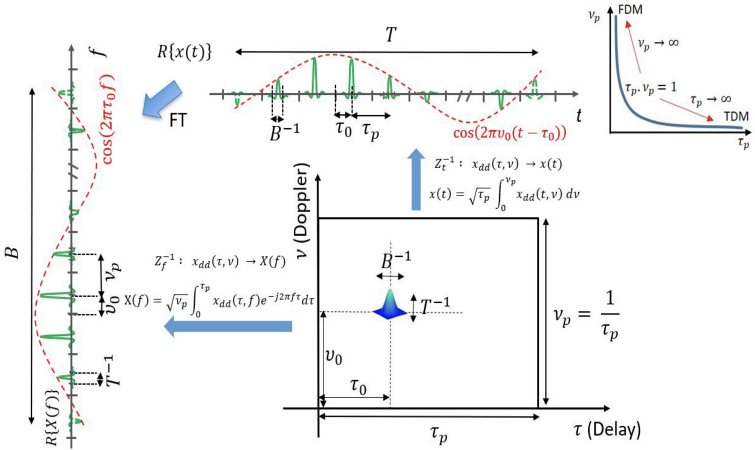

Figure: The TD and FD realizations of a DD pulse are pulse trains modulated by a sinusoid (pulsone). Time duration and bandwidth are inversely related to the spread of the DD pulse along the Doppler and delay axis respectively.

Zak-OTFS modulation

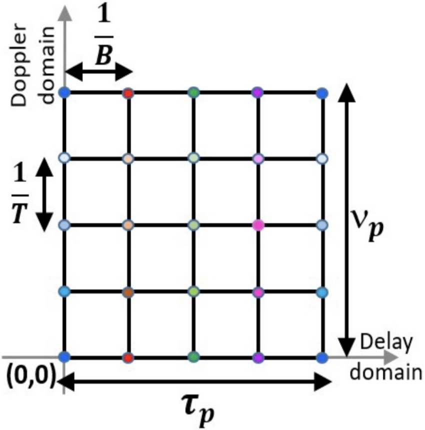

Figure: Information is carried by DD pulses spaced $1/B$ and $1/T$ apart along the delay and Doppler axis respectively (information grid/lattice). $M \triangleq \frac{\tau_p}{1/B}$, $N \triangleq \frac{\nu_p}{1/T}$. No. of carriers is $M\,N = BT$. No loss in dimensionality.

Zak-OTFS - Transceiver Signal Processing

Generating the discrete inf. signal	$x_{\mathrm{dd}}[k+nM, l+mN] \triangleq x[k,l]\, e^{j2\pi n \frac{l}{N}}.$
Generating the analog signal on the information grid	$\Lambda_{\mathrm{dd}} = \left\{ \left(k\frac{\tau_p}{M}, l\frac{\nu_p}{N}\right) \Big\vert\, k,l \in \mathbb{Z} \right\}$ $x_{\mathrm{dd}}(\tau,\nu) = \sum_{k,l\in\mathbb{Z}} x_{\mathrm{dd}}[k,l]\, \delta\left(\tau - k\frac{\tau_p}{M}\right) \delta\left(\nu - l\frac{\nu_p}{N}\right)$
Shaping the pulse at the tx.	$x_{\mathrm{dd}}^{w_{tx}}(\tau,\nu) = w_{tx}(\tau,\nu) *_\sigma x_{\mathrm{dd}}(\tau,\nu)$
Converting to time domain	$s_{\mathrm{td}}(t) = \mathcal{Z}_t^{-1}\left(x_{\mathrm{dd}}^{w_{tx}}(\tau,\nu)\right)$
Applying the channel $h(\tau,\nu)$	$r_{\mathrm{td}}(t) = \iint h_{\mathrm{phy}}(\tau,\nu) s_{\mathrm{td}}(t-\tau)\, e^{j2\pi\nu(t-\tau)}\, d\tau\, d\nu$
Converting to DD domain	$y_{\mathrm{dd}}(\tau,\nu) = \mathcal{Z}_t\left(r_{\mathrm{td}}(t)\right)$
Shaping the pulse at the receiver	$y_{\mathrm{dd}}^{w_{rx}}(\tau,\nu) = w_{rx}(\tau,\nu) *_\sigma y_{\mathrm{dd}}(\tau,\nu)$
Sampling on the information grid	$y_{\mathrm{dd}}[k',l'] = y_{\mathrm{dd}}^{w_{rx}}\left(\tau = k'\frac{\tau_p}{M}, \nu = l'\frac{\nu_p}{N}\right),\ k',l' \in \mathbb{Z}$

$$y_{dd}[k,l] = h_{eff}[k,l] *_\sigma x_{dd}[k,l] = \sum_{k',l'\in\mathbb{Z}} h_{eff}[k',l']\, x_{dd}[k-k', l-l']\, e^{j2\pi \frac{l'(k-k')}{MN}},$$

$$h_{eff}[k,l] = h_{eff}(\tau = k/B, \nu = l/T),\ h_{eff}(\tau,\nu) = w_{rx}(\tau,\nu) *_\sigma h_{\mathrm{phy}}(\tau,\nu) *_\sigma w_{tx}(\tau,\nu)$$

Predictable I/O relation with Zak-OTFS modulation

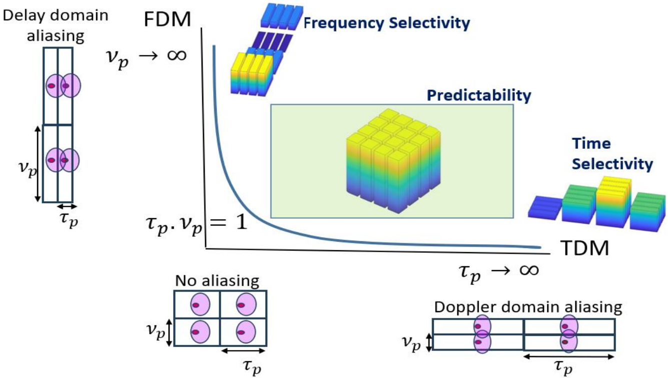

- Channel response to a DD pulse can be measured accurately if channel delay and Doppler spreads are less than respective periods (crystalline regime, no aliasing)
- Channel response to an arbitrary DD pulse can be predicted from the given response to a particular pulse
- In crystalline regime, I/O relation is predictable and non-fading

Other Delay-Doppler Modulation Waveforms

- MC-OTFS (Hadani et. al. WCNC paper 2017): I/O relation is not predictable as it is designed to be compatible with OFDM mod/demod
- Others like AFDM, ODDM, OTSM are also not predictable since the I/O relation is not given by twisted convolution
- Zak-OTFS is predictable since Tx/Rx signal processing acts through twisted convolution just as the LTV channel

Throughput comparison: Zak-OTFS vs. CP-OFDM

- Packet Duration: 1 ms, Bandwidth: 720 KHz
- Total power (Data + pilots) to noise ratio: 12 dB
- Standardized Vehicular-A channel model
- Maximize eff. throughput w.r.t. waveform parameters and adaptive modulation/coding as in 3GPP 5G NR (BLER < 0.1)
- CP-OFDM
  - Sub-carrier spacings: $15, 30, 60$ KHz
  - DMRS (Type-A) boost: $-6, -4, -2, 0, 2, 4, 6$ dB
- Zak-OTFS
  - $\nu_p = 1, 2, 4, 6, 8, 12, 14, 24$ KHz
  - Pilot to data power ratio (PDR) $-10, -5, 0, 5, 10$ dB
  - Gauss-Sinc pulse shaping filters

Throughput comparison: Zak-OTFS vs. CP-OFDM

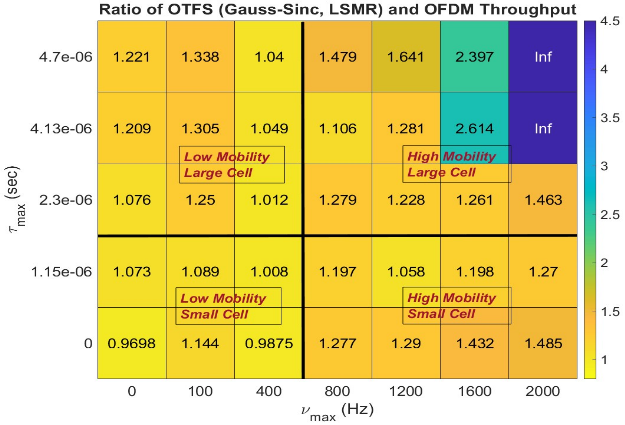

- Zak-OTFS better than CP-OFDM, for both mobility and large cell scenarios
- Gains to be more higher since Zak-OTFS requires almost no re-transmissions due to AWGN like channel
- Significantly better than CP-OFDM for target BLER 10^{-2} (not shown here)

Zak-OTFS based Integrated Sensing and Communication (ISAC)

A Zak-OTFS subframe (point pilot)

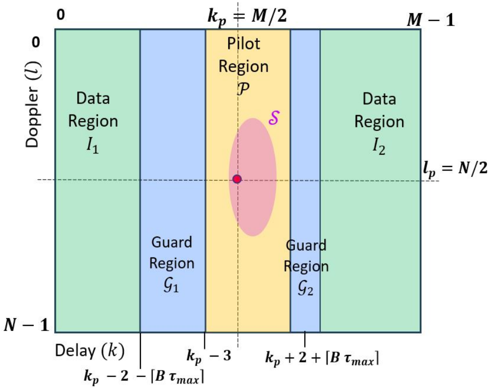

Figure: A Zak-OTFS subframe in DD domain consisting of pilot, guard region and data symbols. Guard regions are overhead.

High PAPR of point pilot

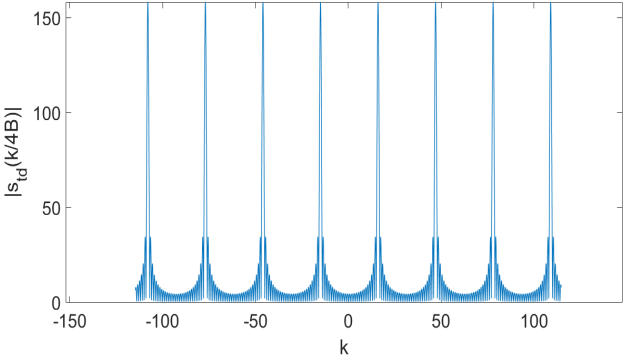

Figure: Tx. TD point pilot signal. High PAPR. $M = 31, N = 37$, $\nu_p = 30$ KHz.

Spread pulsones

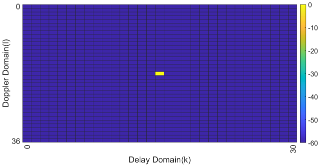

Figure: Point pilot (energy at one point).

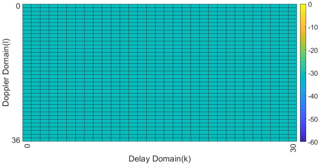

Figure: Spread pilot. Energy is spread using Chirp filter $q = 3$, $M = 31, N = 37$.

- Point pilot at (k_p, l_p)

$$x_{\mathrm{p,dd}}[k,l] = \sum_{n,m\in\mathbb{Z}} e^{j2\pi\frac{nl}{N}}\,\delta[k-k_p-nM]\,\delta[l-l_p-mN]$$

- Spread pilot
  - $x_{\mathrm{s,dd}}[k,l] = w_s[k,l] *_{\sigma} x_{\mathrm{p,dd}}[k,l]$
  - Energy spread over all MN pulsones
  - Energy on each pulsone is $\frac{1}{MN}$

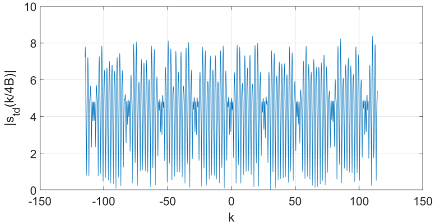

Figure: Tx. TD spread pilot signal. Lower PAPR.

PAPR of spread pulsones

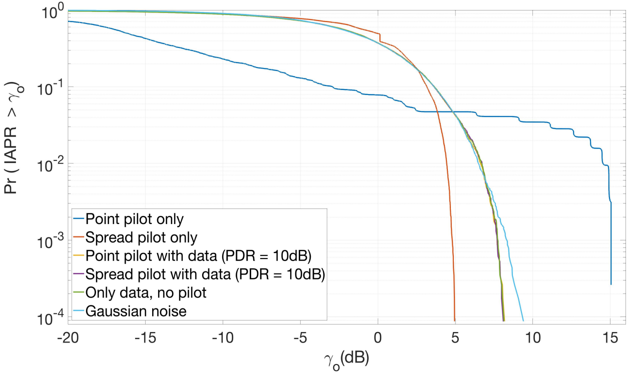

Figure: Complementary CDF (CCDF) plot of IAPR. $M = 31, N = 37$. RRC pulse $w_{tx}(\tau, \nu)$ with roll-off factors, $\beta_\tau = \beta_\nu = 0.6$. Discrete chirp filter with $q = 3$. PDR $\rho_p/\rho_d = 10$ dB. Point pilot PAPR = 15 dB. Spread pilot PAPR is only 5 dB.

Discrete DD domain signals (MN dimensional)

- $M = B\tau_p$, $N = T\nu_p = \frac{T}{\tau_p}$, $MN = BT$
- DD signals are quasi-periodic w.r.t. Λ_{p} but are periodic w.r.t. $\Lambda_{\text{dd}}^{\perp}$

$$x_{\text{dd}}[k + nM, l + mN] = e^{j2\pi \frac{nl}{N}} x_{\text{dd}}[k, l] \;,\; x_{\text{dd}}[k + nMN, l + mMN] = x_{\text{dd}}[k, l]$$

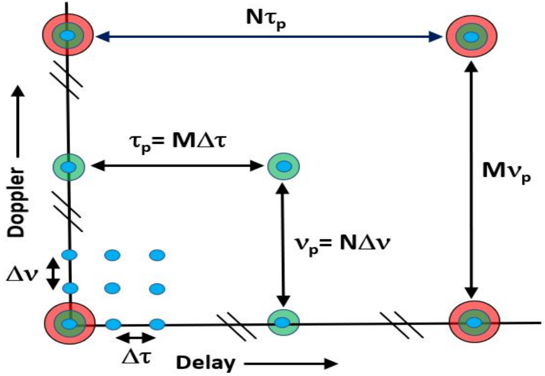

Figure: Information Lattice Λ_{dd} (blue dots), period lattice Λ_{p} (green dots) and the dual of information lattice $\Lambda_{\text{dd}}^{\perp}$ (red dots). $\Delta\tau = \tau_p/M = \frac{1}{B}$ and $\Delta\nu = \nu_p/N = \frac{1}{T}$.

Discrete DD filters are M^2N^2 dimensional

- Filtering of discrete quasi-periodic DD signals ($x_{\mathrm{p,dd}}[k,l]$)
- $*_\sigma$ equivalent to MN-periodic twisted convolution ($\circledast_\sigma$) with MN-periodic extension of filter

$$
\begin{aligned}
x_{\mathrm{s,dd}}[k,l] &\triangleq w_s[k,l] *_\sigma x_{\mathrm{p,dd}}[k,l] \\
&= w[k,l] \circledast_\sigma x_{\mathrm{p,dd}}[k,l] \\
&= \sum_{k'=0}^{MN-1} \sum_{l'=0}^{MN-1} w[k',l']\, x_{\mathrm{p,dd}}[k-k', l-l']\, e^{j2\pi l' \frac{(k-k')}{MN}}
\end{aligned}
$$

- MN-periodic extension of $w_s[k,l]$

$$
w[k,l] \triangleq \sum_{n,m\in\mathbb{Z}} w_s[k+nMN, l+mMN]
$$

- $w[k,l]$ is periodic with period MN, $w[k+nMN, l+mMN] = w[k,l]$
- Response of two discrete filters having the same periodic extension is same
- Discrete filters are $MN \times MN$ dimensional
- Chirp filter $w[k,l] = \frac{1}{MN}\, e^{j2\pi \frac{q(k^2+l^2)}{MN}}$ (q: slope)

Zak-OTFS based Integrated Sensing and Communication

- Transmit signal: data pulsones + spread pulsone (pilot)

$$x_{\text{dd}}[k,l] \;=\; \sqrt{E_d}\, x_{\text{d,dd}}[k,l] + \sqrt{E_p}\, x_{\text{s,dd}}[k,l]$$

- Received signal:

$$\begin{aligned} y_{\text{dd}}[k,l] &= h_{\text{eff}}[k,l] *_{\sigma} x_{\text{dd}}[k,l] + n_{\text{dd}}[k,l] \\ &= \sqrt{E_d}\, \underbrace{\left(h_{\text{eff}}[k,l] *_{\sigma} x_{\text{d,dd}}[k,l]\right)}_{\text{Received data signal}} \\ &\quad + \sqrt{E_p}\, \underbrace{\left(h_{\text{eff}}[k,l] *_{\sigma} x_{\text{s,dd}}[k,l]\right)}_{\text{Received sensing signal}} + n_{\text{dd}}[k,l]. \end{aligned}$$

M. Ubadah, S. K. Mohammed, R. Hadani, S. Kons, A. Chockalingam, and R. Calderbank, "Zak-OTFS for integration of sensing and communication," available online - arXiv:2404.04182v1 [eess.SP], 5 Apr 2024 (http://arxiv.org/abs/2404.04182).

Channel sensing in LTI (Delay-only) channels

- $x[n]$: Discrete-time periodic Tx. pilot signal with period P (continuous time Tx. pilot is time-limited and transmitted with a cyclic prefix)
- Rx. pilot: $y[n] = h[n] \star x[n]$, $\star$: Linear conv., $h[n]$: Channel imp. resp.
- Cross-correlation: Periodic cross-correlation between Rx. and Tx. pilot

$$A_{y,x}[n] \triangleq \sum_{k=0}^{P-1} y[k]\, x^*[k-n] = h[n] \star A_{x,x}[n].$$

- $A_{x,x}[n] \triangleq \sum_{k=0}^{P-1} x[k]\, x^*[k-n]$: Periodic auto-correlation of Tx. pilot
- Ideal auto-correlation: $A_{x,x}[n] = \sum_{k \in \mathbb{Z}} \delta[n-kP]$ (e.g. Zadoff-Chu sequence)

$$A_{y,x}[n] = h[n] \star A_{x,x}[n] = \sum_{k \in \mathbb{Z}} h[n-kP]$$

- **Choose period P to be greater than delay spread of channel $h[n]$**

Channel sensing in LTV channels

- **Tx pilot**: $x_{s,dd}[k,l]$ having discrete-time realization $x_s[n]$ of period $P = MN$ (Discrete Zak-transform)
- **Rx pilot**: $y_{dd}[k,l] = h_{eff}[k,l] *_\sigma x_{s,dd}[k,l]$ having discrete-time realization $y[n]$
- **Cross-ambiguity function** $A_{y,x_s}[k,l]$: **Periodic** cross-correlation between the Rx pilot $y[n]$ and the Tx. pilot delayed by k taps and Doppler shifted by l taps, i.e., $x_s[n-k]\, e^{j2\pi \frac{l(n-k)}{MN}}$

$$A_{y,x_s}[k,l] \;=\; \sum_{n=0}^{MN-1} y[n]\, x_s^*[n-k]\, e^{-j2\pi \frac{l(n-k)}{MN}}$$

- **Cross-ambiguity equiv. computed in discrete DD domain**

$$\begin{aligned} A_{y,x_s}[k,l] &= \sum_{k'=0}^{M-1} \sum_{l'=0}^{N-1} y_{dd}[k',l']\, x_{s,dd}^*[k'-k, l'-l]\, e^{-j2\pi \frac{l(k'-k)}{MN}} \\ &= h_{eff}[k,l] *_\sigma A_{x_s,x_s}[k,l] \end{aligned}$$

- $A_{x_s,x_s}[k,l]$: Cross-ambiguity of the Tx. pilot

Channel sensing with spread pulsone ($q = 5$) ($h_{\text{eff}}[k,l] *_\sigma A_{x_s,x_s}[k,l]$)

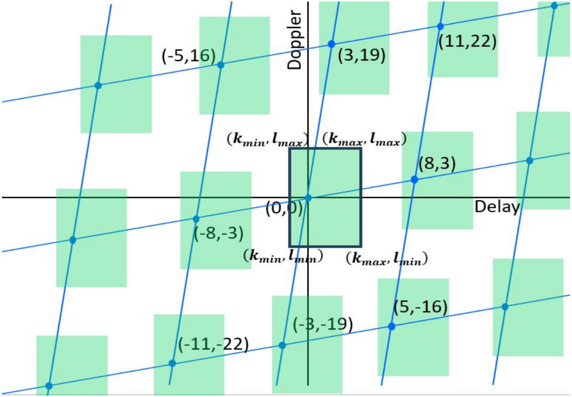

Figure: Blue dots: Lattice type auto-ambiguity of spread pulsone $M = 11, N = 13, q = 5$. $h_{\text{eff}}[k,l]$: Green rectangle with black border. Choice of q such that green rectangles do not overlap. Enables accurate/efficient estimation of $h_{\text{eff}}[k,l]$.

Channel sensing with spread pulsone ($q = 4$) ($h_{\text{eff}}[k, l] *_{\sigma} A_{x_s,x_s}[k, l]$)

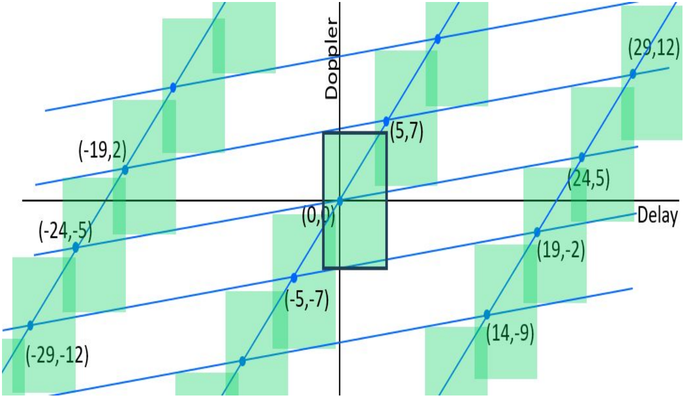

Figure: Chirp filter slope $q = 5 \rightarrow q = 4$. Changes $A_{x_s,x_s}[k, l]$. Support of $h_{\text{eff}}[k, l]$ is same. Green rectangles overlap. Inaccurate estimation of $h_{\text{eff}}[k, l]$.

Channel sensing in a Zak-OTFS ISAC frame

- Received signal

$$y_{\mathrm{dd}}[k,l] = \sqrt{E_d}\,\underbrace{\left(h_{\mathrm{eff}}[k,l] *_\sigma x_{\mathrm{d,dd}}[k,l]\right)}_{\text{Received data signal}} + \sqrt{E_p}\,\underbrace{\left(h_{\mathrm{eff}}[k,l] *_\sigma x_{\mathrm{s,dd}}[k,l]\right)}_{\text{Received sensing signal}} + n_{\mathrm{dd}}[k,l].$$

- Cross-ambiguity between $y_{\mathrm{dd}}[k,l]$ and $x_{\mathrm{s,dd}}[k,l]$

$$A_{y,x_s}[k,l] = \sqrt{E_p}\,h_{\mathrm{eff}}[k,l] *_\sigma A_{x_s,x_s}[k,l] + \underbrace{\sqrt{E_d}\,h_{\mathrm{eff}}[k,l] *_\sigma A_{x_d,x_s}[k,l]}_{\text{data interference to sensing}} + A_{n,x_s}[k,l].$$

- $A_{x_s,x_s}[k,l]$: Auto-ambiguity of tx. spread pilot
- $A_{x_d,x_s}[k,l]$: Cross-ambiguity between tx. data signal and tx. spread pilot
- **Choice of spreading filter** $w[k,l]$: $A_{x_s,x_s}[k,l]$ is almost Dirac-delta (supported on a lattice) and the eff. channel $h_{\mathrm{eff}}[k,l]$ satisfies crystallization condition w.r.t. this lattice, $A_{x_d,x_s}[k,l]$ is noise-like

Channel sensing ($A_{x_d,x_s}[k,l]$)

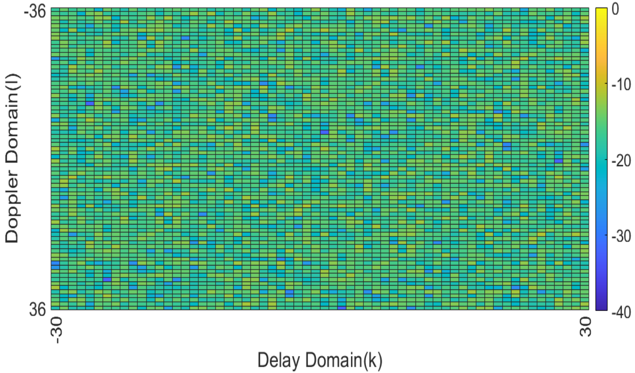

Figure: $|A_{x_d,x_s}[k,l]|$: Magnitude of cross-ambiguity between data and spread pulsone. $E_p = E_d = 1$. $M = 31, N = 37, q = 3$. $|A_{x_d,x_s}[k,l]| \approx \frac{1}{\sqrt{MN}}$. Appears noise-like. Low data to pilot interference.

Joint sensing and communication

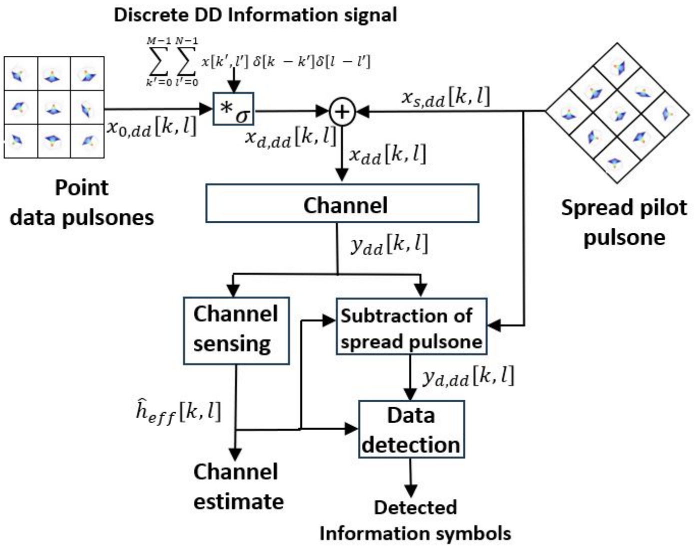

Simulation Parameters

- ITU Veh-A channel model

Path no. i	1	2	3	4	5	6
Rel. Delay τ_i (μs)	0	0.31	0.71	1.09	1.73	2.51
Rel. Power $\frac{\mathbb{E}[\|h_i\|^2]}{\mathbb{E}[\|h_1\|^2]}$ (dB)	0	-1	-9	-10	-15	-20

- Path Doppler shift: $\nu_i = \nu_{max}\cos(\theta_i)$, ν_{max}: Max. path Doppler shift, $\theta_i \sim$ i.i.d. Unif ([0 , 2π)])
- Path channel gain: Rayleigh faded, $\sum_{i=1}^{6} \mathbb{E}[|h_i|^2] = 1$
- Pulse shaping at Tx/Rx: RRC pulses ($\beta_\tau = \beta_\nu = 0.6$), $M = 31, N = 37$, $\nu_p = 30$ KHz. $B = M\nu_p = 0.93$ MHz, $T = N\tau_p = 1.23$ ms
- Received data to noise power ratio: $\rho_d \triangleq \frac{E_d \sum_{(k,l)\in\mathcal{S}} \left|h_{\text{eff}}[k,l]\right|^2}{MNN_0}$
- Received pilot to noise power ratio: $\rho_p \triangleq \frac{E_p \sum_{(k,l)\in\mathcal{S}} \left|h_{\text{eff}}[k,l]\right|^2}{MNN_0}$
- Uncoded 4-QAM BER, DD domain LMMSE equalizer

NMSE (spread pulsone) vs. Pilot to data ratio (PDR)

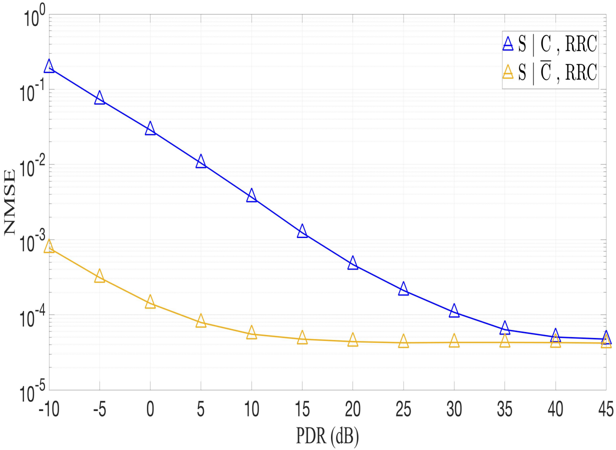

Figure: NMSE vs. PDR for a spread sensing pulsone with $q = 3$. Veh-A channel, RRC pulse shaping filter ($\beta_\tau = \beta_\nu = 0.6$), data SNR $\rho_d = 25$ dB, $\nu_{max} = 815$ Hz, $\nu_p = 30$ KHz, $M = 31, N = 37$. Flooring at high PDR is due to DD domain aliasing.

BER vs. PDR ("U" shaped)

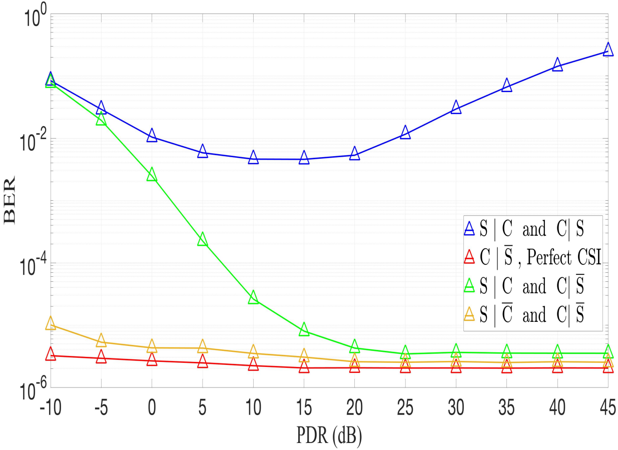

Figure: BER vs. PDR for a spread sensing pulsone with $q = 3$. Veh-A channel. RRC pulse shaping filter ($\beta_\tau = \beta_\nu = 0.6$), data SNR $\rho_d = 25$ dB, $\nu_{max} = 815$ Hz, $\nu_p = 30$ KHz, $M = 31, N = 37$. BER improves with increasing PDR and then degrades with further increase due to increase in residual pilot after cancellation.

BER vs. ν_{max}

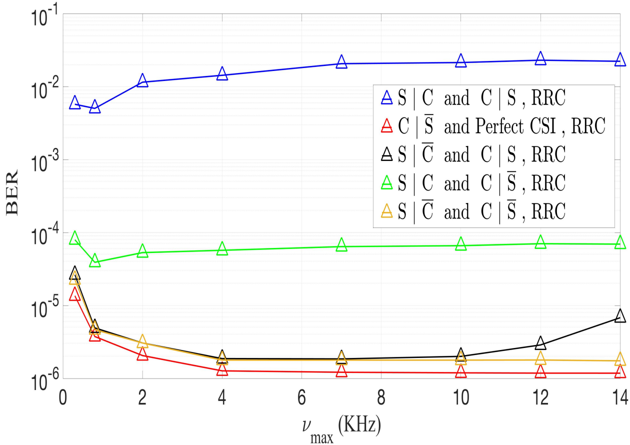

Figure: BER vs ν_{max} for spread sensing pulsone ($q = 3$). Veh-A channel model, RRC pulse shaping filter ($\beta_\tau = \beta_\nu = 0.6$), Doppler period $\nu_p = 30$ KHz, PDR $\frac{\rho_p}{\rho_d} = 10$ dB, data SNR $\rho_d = 25$ dB. BER almost invariant of Doppler spread in crystalline regime ($2\nu_{max} < \nu_p$). Gap in performance w.r.t. perfect CSI.

Throughput vs. ν_{max}

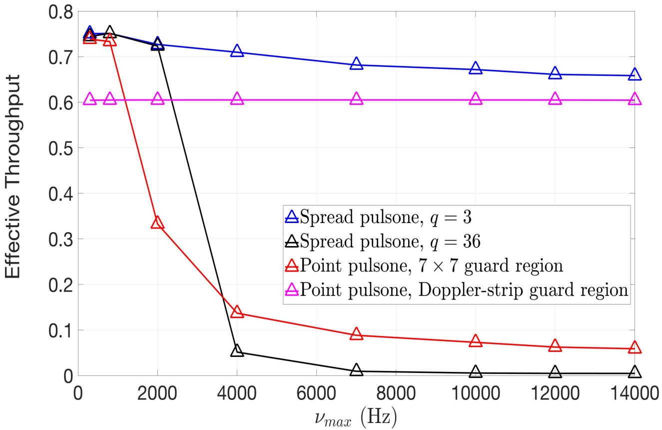

Figure: Effective throughput (bits/sec/Hz) as a function of increasing ν_{max}. Integrated sensing and communication (**S**| **C** & **C**|**S**). $\nu_p = 30$ KHz. $M = 31, N = 37$. RRC pulse shaping filter ($\beta_\tau = \beta_\nu = 0.6$). Spread pilot results in higher effective throughput.

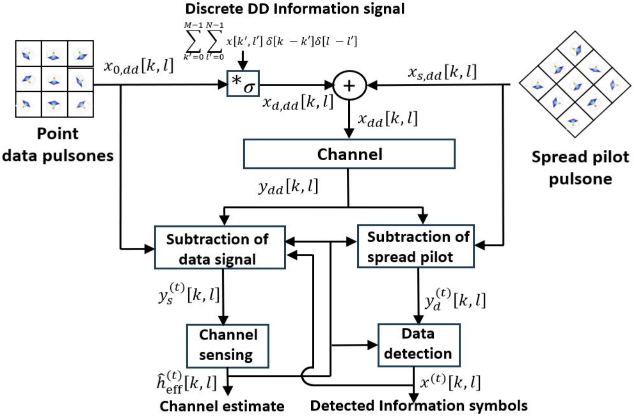

Figure: Signal processing for proposed Zak-OTFS based iterative joint sensing and communication.

BER with Turbo signal processing

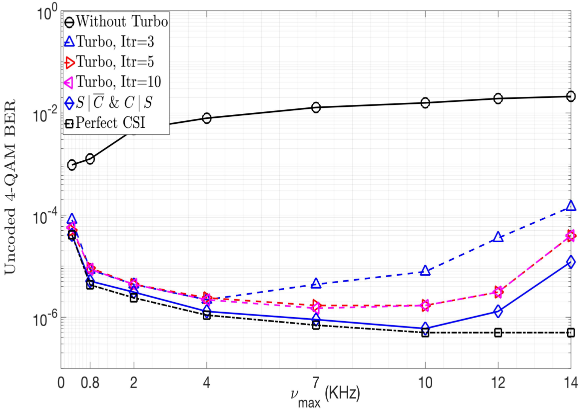

Figure: Veh-A channel, data SNR = 25 dB, PDR = 10 dB. With turbo iterations BER is close to that with perfect CSI.

Zak-OTFS Radar

(Lines vs. Lattices)

Zak-OTFS Radar

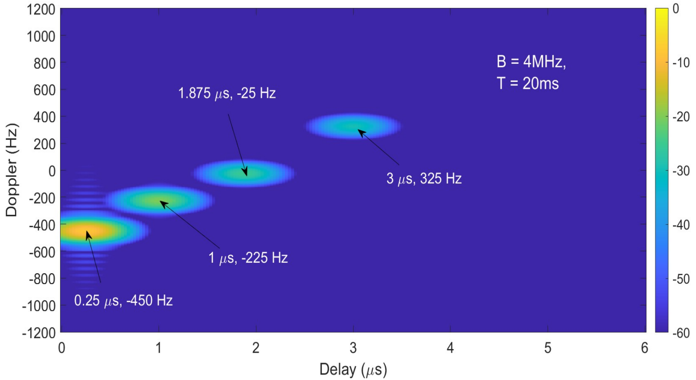

- Tx. radar signal (DD pulse) is at origin.
- Very simple detection. The DD shift of each received pulse (relative to the origin) is an estimate of the target's distance and velocity.
- Complexity is only that of TD $\rightarrow$ DD (Zak transform) $O(BT\ \log(BT))$

Table: Comparison with prior works on identification of linear time-varying systems with $K > 1$ targets. $\Delta\tau$ and $\Delta\nu$ are the delay and Doppler domain resolution respectively.

Identification approach	Min. reqd. time-bandwidth (BT)	Complexity	Resolution
Compressive sensing based	K^2	$O(K^3)$	$\Delta\tau \propto \frac{1}{B}$ $\Delta\nu \propto \frac{1}{T}$
Super-resolution (MUSIC)	K^2	$O(K^3)$	Infinite
DD domain Cross-ambiguity Chirp (LFM) pulses Section III in [8]	$4K$	K^2	$\Delta\nu \propto \frac{4}{T}$ $\Delta\tau \propto \frac{1}{B}$
DD domain Cross-ambiguity Zak-OTFS pulsone Section IV in [8]	K	$K \log K$	$\Delta\nu \propto \frac{1}{T}$ $\Delta\tau \propto \frac{1}{B}$

Chirps (LFM) - Single target

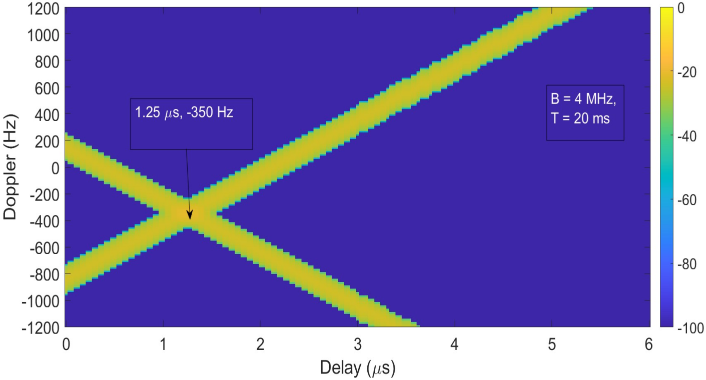

- Chirp $e^{j\pi a t^2}$ has auto-ambiguity function supported on the line $\nu - a\tau = 0$ in DD domain
- Need two chirps to localize a single target

Chirps - Multiple target

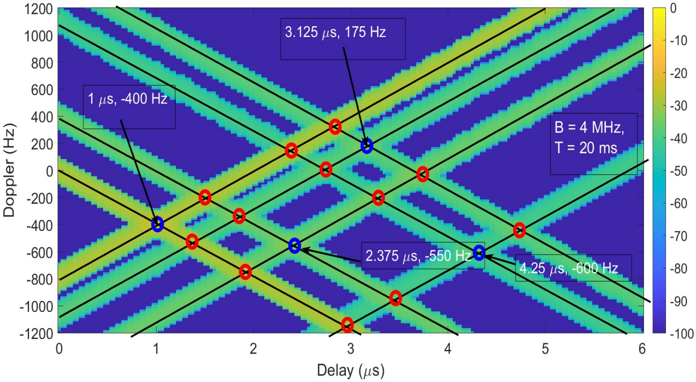

- Multiple targets: more intersections than the no. of true targets, issue of "ghost" targets
- Need at least two-pairs of up-chirp-/down-chirp of different slopes to resolve multiple target (loss in Doppler resolution)

Chirps vs Zak-OTFS

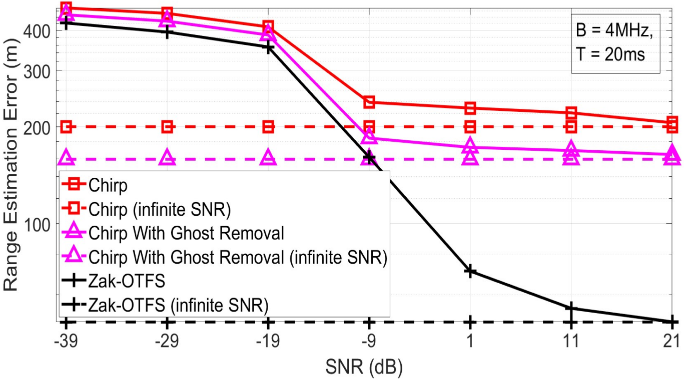

- Four targets unif. dist. in the DD rectangle $[0\,,\,3]\mu s \times [-600\,,\,600]$ Hz.
- Zak-OTFS with $\tau_p = 100\,\mu s$ and $\nu_p = 10$ KHz. Gaussian pulse shaping.
- RMS range est. error is smaller with Zak-OTFS than with Chirps

References

1. `https://sites.google.com/view/prof-saif-khan-mohammed/research`
2. S. K. Mohammed,"Derivation of OTFS Modulation From First Principles," *IEEE Transactions on Vehicular Technology*, vol. 70, no. 8, pp. 7619-7636, Aug. 2021.
3. S. K. Mohammed, "Time-Domain to Delay-Doppler Domain Conversion of OTFS Signals in Very High Mobility Scenarios," *IEEE Trans. on Vehicular Technology*, vol. 70, no. 6, pp. 6178-6183, June 2021.
4. S. K. Mohammed, R. Hadani, A. Chockalingam and R. Calderbank, "OTFS – A Mathematical Foundation for Communication and Radar Sensing in the Delay-Doppler Domain," *IEEE BITS the Information Theory Magazine*, 2022, doi: 10.1109/MBITS.2022.3216536. arXiv:2302.08696 [eess.SP]
5. S. K. Mohammed, R. Hadani, A. Chockalingam and R. Calderbank, "OTFS - Predictability in the Delay-Doppler Domain and its Value to Communication and Radar Sensing," *IEEE BITS the Information Theory Magazine*, vol. 3, no. 2, pp. 7 - 31, June 2023. arXiv:2302.08705 [eess.SP]
6. M. Ubadah, S. K. Mohammed, R. Hadani, S. Kons, A. Chockalingam, and R. Calderbank, "Zak-OTFS for integration of sensing and communication," available online - arXiv:2404.04182v1 [eess.SP], 5 Apr 2024 (http://arxiv.org/abs/2404.04182).
7. J. Jayachandran, M. Ubadah, S. K. Mohammed, R. Hadani, A. Chockalingam, and R. Calderbank, "Zak-OTFS and Turbo Signal Processing for Joint Sensing and Communication," *available online*, June 2024 (https://arxiv.org/abs/2406.06024).
8. D. Nisar, S. K. Mohammed, R. Hadani, A. Chockalingam, R. Calderbank, "Zak-OTFS for Identification of Linear Time-Varying Systems," *available online*, March 2025 (https://arxiv.org/abs/2503.18900).

Thank you

Zak-OTFS - Transceiver signal processing

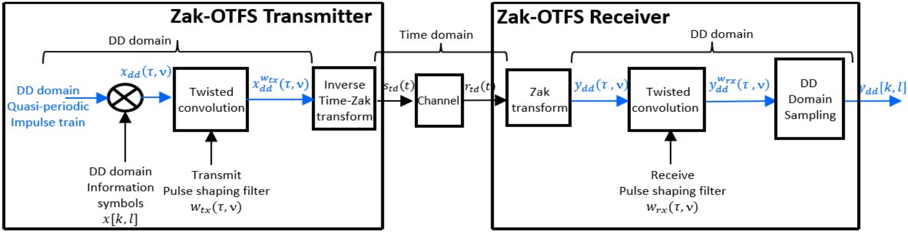

- Channel acts through twisted convolution ($*_\sigma$): $y_{dd}(\tau,\nu) = h(\tau,\nu) *_\sigma x_{dd}^{w_{tx}}(\tau,\nu)$
- Input-Output (I/O) relation: $y_{dd}^{w_{rx}}(\tau,\nu) = h_{eff}(\tau,\nu) *_\sigma x_{dd}(\tau,\nu)$
- Effective DD channel: $h_{eff}(\tau,\nu) = w_{rx}(\tau,\nu) *_\sigma h(\tau,\nu) *_\sigma w_{tx}(\tau,\nu)$
- Sampled I/O relation: $y_{dd}[k,l] = y_{dd}^{w_{rx}}\left(\tau = \frac{k\tau_p}{M}, \nu = \frac{l\nu_p}{N}\right) = h_{eff}[k,l] *_\sigma x_{dd}[k,l]$
- DD domain I/O relation is stationary/predictable if $h_{eff}[k,l]$ is known/can be acquired efficiently
- Model-free approach: acquire $h_{eff}[k,l]$ and not $h(\tau,\nu)$